

1 Direct Detection of Dark Matter

In the past two decades, a standard cosmological picture of the universe (the Lambda Cold Dark Matter or LCDM model) has emerged, which includes a detailed breakdown of the main constituents of the energy density of the universe. This theoretical framework is now on a firm empirical footing, given the remarkable agreement of a diverse set of astrophysical data [1,2]. Recent results by Planck largely confirm the earlier Wilkinson Microwave Anisotropy Probe (WMAP) conclusions and show that the universe is spatially flat, with an acceleration in the rate of expansion and an energy budget comprising ~5% baryonic matter, ~26% cold dark matter (CDM), and roughly ~69% dark energy [3,4]. With the generation-2 (G2) dark-matter experiments, we are now in a position to identify this dark matter through sensitive terrestrial *direct detection* experiments. Failing to detect a signal in the next (or subsequent generation [G3] of experiments) would rule out most of the natural parameter space that describes weakly interacting massive particles (WIMPs), forcing us to reassess the WIMP paradigm and look for new detection techniques. In the following sections, we introduce the cosmological and particle physics evidence pointing to the hypothesis that the dark matter is composed of WIMPs, detectable through nuclear recoil (NR) interactions in low-background experiments. We then give the motivation for a very massive liquid xenon (LXe) detector as the logical next step in the direct detection of dark matter.

1.1 Cosmology and Complementarity

While the Large Hadron Collider (LHC) experiments continue to verify the Standard Model of particle physics to ever-greater precision, the nature of the particles and fields that constitute dark energy and dark matter remains elusive. The gravitational effects of dark matter are evident throughout the cosmos, dominating gravitational interactions of objects as small as dwarf satellites of the Milky Way, up to galaxy clusters and superclusters. Simple application of Kepler's laws leads to the inescapable conclusion that our own galaxy (and all others) are held together by the gravitational pull of a dark halo that outweighs the combined mass of stars and gas by an order of magnitude, and appears to form an extended halo beyond the distribution of luminous matter.

At the same time, very weakly interacting CDM (particles or compact objects that were moving non-relativistically at the time of decoupling) appears to be an essential ingredient in the evolution of structure in the universe. N-body simulations of CDM can explain much of the structure, ranging from objects made of tens of thousands of stars to galaxy clusters. In the past few years, more realistic simulations, including both baryonic matter (gas and stars) and dark matter, are beginning to reveal how galaxy-like objects can arise from the primordial perturbations in the early universe [5,6]. While we know much about the impact of dark matter on a variety of astrophysical phenomena, we know very little about its nature.

An attractive conjecture is that dark-matter particles were in equilibrium with ordinary matter in the hot early universe. We note, however, that there are viable dark-matter candidates, including axions, where the conjecture of thermal equilibrium is not made [7]. Thermal equilibrium describes the balance between annihilation of dark matter into ordinary particle-antiparticle pairs, and vice versa. As the universe expanded and cooled, the reaction rates (the product of number density, cross section, and relative velocity) eventually fell below the level required for thermal equilibrium, leaving behind a relic abundance of dark matter. The lower the annihilation cross section of dark matter into ordinary matter, the higher the relic abundance of dark matter. An annihilation cross-section characteristic of the weak interaction results in a dark-matter energy consistent with that observed by cosmological measurements [8].

Remarkably, models of supersymmetry (SUSY) predict the neutralino, a new particle that has properties appropriate to be a WIMP. SUSY posits a fermion-like partner for every Standard Model boson, and a boson-like partner for every Standard Model fermion. A principal feature of SUSY is its natural means

for achieving cancellations in quantum field theory amplitudes that could cause the Higgs mass to be much higher than the $125 \text{ GeV}/c^2$ recently observed [9,10]. The neutralino is a coherent quantum state formed from the SUSY partners of the photon, the Z^0 , and Higgs boson, and is a “Majorana” particle, meaning it is its own antiparticle.

Astrophysical measurements show that dark matter behaves like a particle and not like a modification of gravity. Gravitational lensing of distant galaxies by foreground galactic clusters can provide a map of the total gravitational mass, showing that this mass far exceeds that of ordinary baryonic matter. By combining the distribution of the total gravitational mass (from lensing) with the distribution of the dominant component of baryonic matter (evident in the X-ray-emitting cluster gas) one can see whether the dark mass follows the distribution of baryonic matter. For some galaxy clusters, in particular the Bullet cluster [11], the total gravitational mass (dominated by dark matter) follows the distribution of other non-interacting test particles (stars) rather than the dominant component of baryonic matter in the cluster gas. Combining this evidence with other observations of stellar distributions and velocity measurements for galaxies with a wide range of mass-to-light ratios, it appears that the total gravitational mass does not follow the distribution of baryonic matter as one would expect for modified gravity, but behaves like a second, dark component of relatively weakly interacting particles.

There are three complementary signals of WIMP dark matter. The dark matter of the Milky Way can interact with atomic nuclei, resulting in NRs that are the basis of direct detection (DD) experiments like LZ. At the LHC, the dark matter will appear as a stable, non-interacting particle that causes missing energy and momentum. Out in the cosmos, dark matter collects at the centers of galaxies and in the sun, where pairs of dark-matter particles will annihilate with one another, if the dark matter is a Majorana particle, as expected in SUSY theories. The annihilations will produce secondary particles, including positrons, antiprotons, neutrinos, and gamma rays, providing the basis for “indirect” detection (ID) by gamma ray, cosmic ray, and neutrino telescopes.

In Figure 1.1.1, we show the results of a recent analysis of the complementarity of the three signals from WIMP dark matter. The LHC has already provided constraints on the simplest SUSY parameter space, and the Higgs mass is in some tension with the most constrained versions of SUSY, requiring theorists to relax simplifying assumptions. One slightly less restrictive choice of parameters is the so-called phenomenological minimal supersymmetric standard model (pMSSM) model [12,13]. In Figure 1.1.1, each point represents a choice of pMSSM parameters that satisfies all known physics and astrophysics constraints [14]. The color of the points show which experiments have adequate sensitivity to test

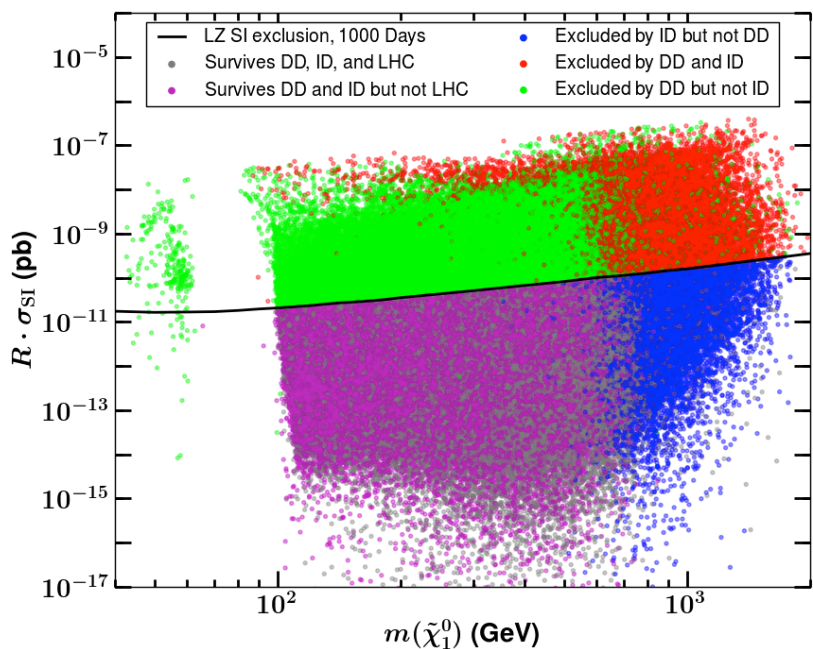


Figure 1.1.1. Scan of pMSSM parameter space and complementarity. Each point in this space of the cross section, scaled by abundance, of WIMPs with nucleons versus mass of the WIMP represents a SUSY model. The colors show models that can be tested by the three techniques of detection: direct detection (DD), LHC, and indirect detection (ID), and their combinations. The expected LZ sensitivity is shown as the black line [14].

whether that point is valid. The three experimental tests are: DD with the proposed LZ experiment, current LHC data, and ID from a proposed ID experiment (an enhanced version of the Cherenkov Telescope Array [15] with twice the number of telescopes compared with the current baseline). Each of the three experimental techniques tends to be most sensitive to one region in Figure 1.1.1, although there are regions of overlapping sensitivity.

The three experimental techniques are subject to very different systematic limitations. Direct-detection experiments like LZ depend on the extrapolation of interaction cross sections from Big Bang conditions to the current astrophysical situation, but are relatively free from uncertainty due to imperfect knowledge of the local mass density of dark matter. The LHC production of dark matter also depends on specific implementation of the processes that mediate dark-matter creation, but can have sensitivity down to the zero WIMP mass. Indirect detection signals depend sensitively on the assumed density of dark matter in astrophysical sources, but the annihilation cross section is closely related to the decoupling cross section.

The most important goal for the G2 program is to produce the best constraints over the natural mass range for dark matter. The LZ experiment accomplishes this goal. A broader goal of dark-matter research is to use the three complementary approaches to establish the validity of any signal, and to identify the properties of the dark-matter particle. For example, if LZ first sees a signal, ID could follow up with measurements of the gamma-ray spectrum and angular distribution that aid in determining the mass, annihilation channels, and galactic dark-matter halo density, and the LHC or future colliders could fully explore the nature of the dark-matter particle through experiments that actually create it in the laboratory.

1.2 Direct Detection Experiments

The direct detection of dark matter in earthbound experiments depends on the local properties of the Milky Way's dark matter and on the properties of the dark-matter particles themselves. The local properties of the Milky Way's dark halo are determined by astrophysical studies, and include the local dark-matter mass density as well as the distribution of the velocities of dark-matter particles. The conjecture that the dark-matter particles are WIMPs implies that its scattering with the nucleus is non-relativistic two-body scattering; in LZ, we seek to observe the xenon nuclei that recoil after having been struck by an incoming WIMP. The mass assumed for the WIMP determines the kinematics of the scattering, and the rate of WIMP-nucleus scatters seen in a WIMP detector depends additionally on the exposure defined as the product of the target mass and the live time, the WIMP-nucleus cross section, and the energy threshold for detection of the NR.

The dark-matter halo of the Milky Way is harder to quantify than that of other galaxies. The density of all matter, including dark matter, in galaxies is quantified with rotation curves, which describe the average circular velocity of matter in orbit about the galactic center as a function of radius from the galactic center. The rotation curve of the Milky Way for radii larger than 8.0 kpc, that of our sun, is a challenge to quantify. Estimates of the local dark-matter density range from $0.235 \pm 0.030 \text{ GeV/cm}^3$ to $0.389 \pm 0.025 \text{ GeV/cm}^3$ [16-18]. Most DD experiments adopt, for ease of inter-comparison, a standard value for the local dark-matter mass density of $\rho_0=0.3 \text{ GeV/cm}^3$. The experiments also adopt a standard distribution function for the velocity of dark-matter particles, characterized by a Maxwell-Boltzmann distribution with solar circular velocity $v_0=220 \text{ km/s}$, which is cut off at the galactic escape velocity of $v_{\text{esc}}=544 \text{ km/s}$, and with proper accounting for the sun's peculiar velocity and the periodic annual motion of the Earth [19,20].

The minimum WIMP mass detectable with a particular DD experiment depends on the maximum velocity in the galactic WIMP spectrum, the atomic mass A of the target nucleus, and the energy threshold E_{min} for NR detection in that experiment. Straightforward kinematics gives the minimum detectable WIMP mass as $M_{\text{WIMP}}(\text{GeV}) \approx (1/4)\sqrt{E_{\text{min}}(\text{keV})A}$, for a maximum velocity of $v_{\text{esc}}=544 \text{ km/s}$. This minimum M_{WIMP} is 2 GeV for the recent CDMSlite Ge-target result [21], and 6 GeV for the recent LUX result [22] using LXe.

These results are shown in Figure 1.2.1, from Ref. [23], along with the current experimental situation for the spin-independent (SI) WIMP-nucleon cross section. We discuss the details of spin independence and other types of WIMP-nucleon interactions in Chapter 4. The SI cross section is the standard benchmark, and would result from a WIMP coupling to the Standard Model Higgs.

As the presumed M_{WIMP} rises above this value, the portion of the WIMP velocity distribution that permits NR above the detectable threshold rises rapidly. This rapid rise drives the improvement in sensitivities as M_{WIMP} rises above 5 GeV, as shown in Figure 1.2.1. As M_{WIMP} approaches the mass of the atom used in the target, the kinematics of energy transfer to the target nuclei becomes most efficient, and experiments reach their maximum sensitivity.

This region, roughly $M_{\text{WIMP}} > 10$ GeV, is the region most likely for a WIMP, as other weak-interaction particles, including the Z^0 , the W , and the Higgs particles, have masses in that region. As M_{WIMP} grows yet larger, the number density of WIMPs implied by the astrophysical mass density, $0.3/M_{\text{WIMP}}(\text{GeV}) \text{ 1/cm}^3$, falls, reducing the sensitivity of direct-detection experiments, as shown in Figure 1.2.1. The maximum WIMP mass consistent with thermal equilibrium in the early universe is 340 TeV, above which unitarity can no longer be satisfied [24].

Figure 1.2.1 also shows a number of closed “regions of interest” from a variety of experiments, which indicate potential signals. All of the regions of interest result from excesses of events just above the thresholds of the respective experiments, where backgrounds are in general the highest and most challenging to understand thoroughly. The most robust regions of interest are those from the DAMA/LIBRA collaboration, which employed most recently 250 kg of sodium iodide crystals for a total exposure of 1.17 tonne-years [25].

The DAMA/LIBRA experiment sought an effect caused by the Earth’s orbit about the sun. In June of each year, the Earth’s orbital velocity adds to that of the sun’s circular velocity around the center of the Milky Way, and in December of each year the Earth’s orbital velocity cancels a small portion of the sun’s circular velocity. The number of events just above threshold seen by DAMA increases in June, and was diminished in December; the strength of DAMA/LIBRA’s signal is 8.9 standard deviations. Detailed criticisms of the DAMA/LIBRA result are presented in Ref. [23]. As can be seen from Figure 1.2.1, results from experiments that use Ge targets (CDMS and EDELWEISS) or Xe targets (ZEPLIN-III,

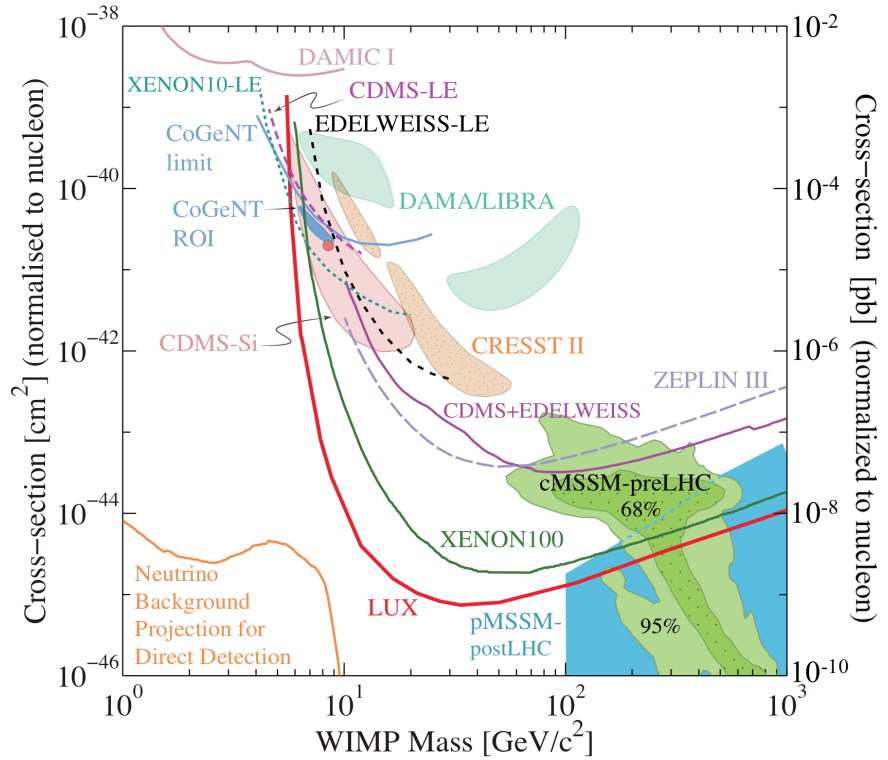


Figure 1.2.1. A compilation of current WIMP-nucleon SI cross-section upper limits at 90% confidence level (solid and dashed curves, labeled by experiment names), and hints for WIMP signals (pale shaded closed contours, labeled by experiment names). Regions favored by supersymmetric models are the bold closed curves at the lower right. From Ref. [23].

XENON100, and LUX) have attained sensitivities that exceed those of DAMA/LIBRA by many orders of magnitude, under the most simple SI interpretation.

The history of and future projections for WIMP sensitivity are shown in Figure 1.2.2. There are three distinct eras: (1) 1986-1996; (2) 2000-2010; and (3) post-2010. In the first era, low-background Ge and NaI crystals dominated. In these experiments, discrimination between the dominant background of electron recoils (ERs) from gamma rays and NRs was not available. The cross-section sensitivity per nucleon achieved, 10^{-41} cm^2 (10^{-5} pb), was sufficient to rule out the most straightforward WIMP

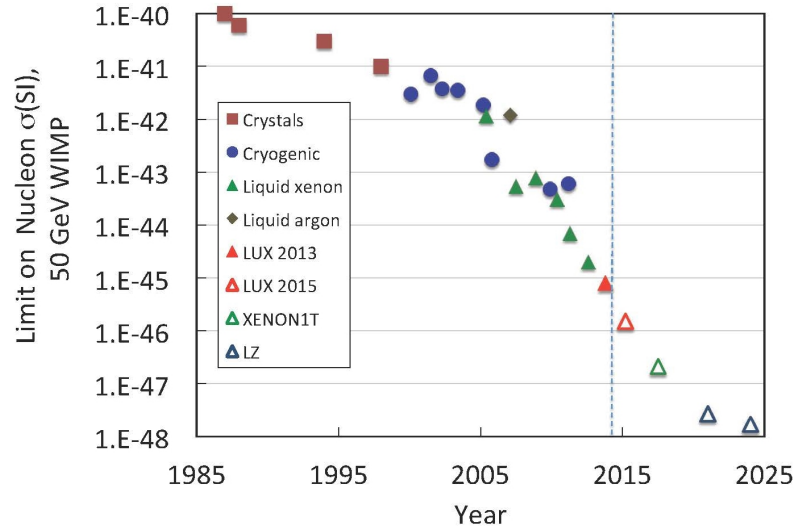


Figure 1.2.2. The evolution of cross-section limit for 50 GeV WIMPs as a function of time. Past points are published results. Future points are from the Snowmass meetings [26].

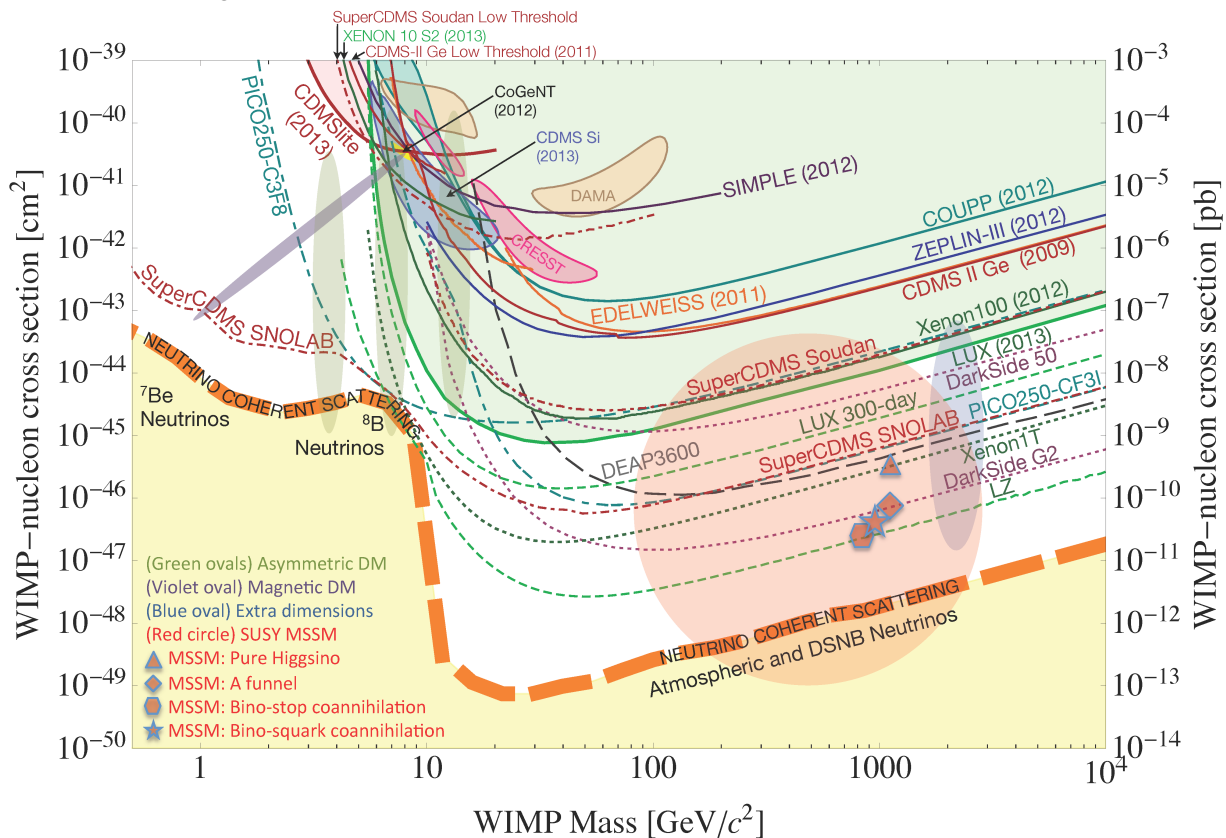


Figure 1.2.3. A compilation of WIMP-nucleon SI cross-section sensitivity (solid curves), hints for WIMP signals (shaded closed contours), and projections (dot and dot-dash curves) for DD experiments of the past and projected into the future. Also shown is an approximate band where the coherent nuclear scattering of ^8B solar neutrinos, atmospheric neutrinos, and diffuse supernova neutrinos will limit the sensitivity of DD experiments to WIMPs. Finally, a suite of theoretical model predictions is indicated by the shaded regions, with model references included [26].

implementation: that the WIMP is a heavy Dirac neutrino, which was the original suggestion of Ref. [8]. In the second era, cryogenic Ge detectors with the ability to distinguish NR from the ER background dominated, and achieved a cross-section per nucleon sensitivity of $5 \times 10^{-44} \text{ cm}^2$ ($5 \times 10^{-8} \text{ pb}$). This sensitivity began to probe dark matter that is a Majorana fermion, which couples to nucleons via the Higgs particle. In the third era, still under way, LXe time projection chambers (TPCs) have been most sensitive, and with the LUX experiment have achieved a sensitivity of $7.6 \times 10^{-46} \text{ cm}^2$ ($7.6 \times 10^{-10} \text{ pb}$). The LXe TPC has the ability to discriminate ER and NR, and can be expanded to large, homogenous volumes. It is possible to make accurate predictions for the backgrounds in the central LXe TPC region, particularly with the added power of outer detectors that can characterize the radiation field in the TPC vicinity.

A more detailed portrayal of the variety of experiments, both from the past and projected into the future, is given in Figure 1.2.3 [26]. In the region $M_{\text{WIMP}} > 10 \text{ GeV}$, most likely for a WIMP due to proximity to the masses of the weak bosons, LZ will be the most sensitive experiment. Figure 1.2.3 also shows the “neutrino floor,” where NRs from coherent neutrino scattering, a process that has not yet been observed, will greatly influence progress in sensitivity to WIMP interactions. A 1,000-day run of the LZ experiment will just begin to touch this background. Searches for direct interactions of dark matter with exposure substantially greater than LZ will see many candidate events from NRs in response to, primarily, atmospheric neutrinos.

Chapter 1 References

- [1] D. N. Spergel *et al.* (WMAP), *Astrophys. J. Suppl.* **170**, 377 (2007), arXiv:astro-ph/0603449 [astro-ph].
- [2] W. J. Percival *et al.*, *Astrophys. J.* **657**, 645 (2007), arXiv:astro-ph/0608636 [astro-ph].
- [3] E. Komatsu *et al.* (WMAP), *Astrophys. J. Suppl.* **192**, 18 (2011), arXiv:1001.4538 [astro-ph].
- [4] P. A. R. Ade *et al.* (Planck), *Astron. Astrophys.* **571**, A16 (2014), arXiv:1303.5076 [astro-ph].
- [5] C. S. Frenk and S. D. M. White, *Ann. Phys. (Berlin)* **524**, 507 (2012), arXiv:1210.0544 [astro-ph].
- [6] F. Governato, A. Zolotov, A. Pontzen, C. Christensen, S. H. Oh, A. M. Brooks, T. Quinn, S. Shen, and J. Wadsley, *Mon. Not. R. Astron. Soc.* **422**, 1231 (2012), arXiv:1202.0554 [astro-ph].
- [7] A. Kusenko and L. J. Rosenberg, in *Planning the Future of U.S. Particle Physics, The Snowmass 2013 Proceedings*, edited by N. A. Graf, M. E. Peskin, and J. L. Rosner (2013); Working Group Report: *Non-WIMP Dark Matter*, arXiv:1310.8642 [hep-ph].
- [8] B. W. Lee and S. Weinberg, *Phys. Rev. Lett.* **39**, 165 (1977).
- [9] G. Aad *et al.* (ATLAS), *Phys. Lett.* **B716**, 1 (2012), arXiv:1207.7214 [hep-ex].
- [10] S. Chatrchyan *et al.* (CMS), *Phys. Lett.* **B716**, 30 (2012), arXiv:1207.7235 [hep-ex].
- [11] D. Clowe, M. Bradac, A. H. Gonzalez, M. Markevitch, S. W. Randall, C. Jones, and D. Zaritsky, *Astrophys. J.* **648**, L109 (2006), arXiv:astro-ph/0608407 [astro-ph].
- [12] A. Djouadi *et al.* (MSSM Working Group), in *GDR (Groupement de Recherche) - Supersymétrie Montpellier, France, April 15-17, 1998* (1998) arXiv:hep-ph/9901246 [hep-ph].
- [13] C. F. Berger, J. S. Gainer, J. L. Hewett, and T. G. Rizzo, *J. High Energy Phys.* **2009**, 023 (2009), arXiv:0812.0980 [hep-ph].
- [14] M. Cahill-Rowley, R. Cotta, A. Drlica-Wagner, S. Funk, J. Hewett, A. Ismail, T. Rizzo, and M. Wood, *Phys. Rev.* **D91**, 055011 (2015), arXiv:1405.6716 [hep-ph].
- [15] B. S. Acharya *et al.*, *Astropart. Phys.* **43**, 3 (2013).
- [16] Y. Sofue, *Publ. Astron. Soc. Jap.* **64**, 75 (2012), arXiv:1110.4431 [astro-ph].
- [17] J. Bovy and S. Tremaine, *Astrophys. J.* **756**, 89 (2012), arXiv:1205.4033 [astro-ph].
- [18] R. Catena and P. Ullio, *J. Cosmol. Astropart. Phys.* **2010**, 004 (2010), arXiv:0907.0018 [astro-ph].
- [19] K. Freese, J. A. Frieman, and A. Gould, *Phys. Rev.* **D37**, 3388 (1988).
- [20] C. Savage, K. Freese, and P. Gondolo, *Phys. Rev.* **D74**, 043531 (2006), arXiv:astro-ph/0607121 [astro-ph].
- [21] R. Agnese *et al.* (SuperCDMS), *Phys. Rev. Lett.* **112**, 041302 (2014), arXiv:1309.3259 [physics.ins-det].
- [22] D. S. Akerib *et al.* (LUX), *Phys. Rev. Lett.* **112**, 091303 (2014), arXiv:1310.8214 [astro-ph].
- [23] K. A. Olive *et al.* (Particle Data Group), *Chin. Phys.* **C38**, 090001 (2014), Review of Particle Physics: *Astrophysics and Cosmology*, M. Drees and G. Gerbier, *Dark Matter*, pp. 353-360.
- [24] K. Griest and M. Kamionkowski, *Phys. Rev. Lett.* **64**, 615 (1990).
- [25] R. Bernabei *et al.* (DAMA, LIBRA), *Eur. Phys. J.* **C67**, 39 (2010), arXiv:1002.1028 [astro-ph].
- [26] P. Cushman *et al.*, in *Planning the Future of U.S. Particle Physics, The Snowmass 2013 Proceedings*, edited by N. A. Graf, M. E. Peskin, and J. L. Rosner (2013); Working Group Report: *WIMP Dark Matter Direct Detection*, arXiv:1310.8327 [hep-ex].